

SUPPRESSION OF 3D FLOW INSTABILITIES IN TIGHTLY PACKED TUBE BUNDLES

N. K.-R. Kevlahan

Department of Mathematics & Statistics, McMaster University, Hamilton, Canada

J. Simon

École MatMéca, Bordeaux, France

N. Tonnet

École MatMéca, Bordeaux, France

J. Wadsley

Department of Physics & Astronomy, McMaster University, Hamilton, Canada

ABSTRACT

We study the generation of three-dimensional vorticity in tightly packed tube bundles. In particular, our goal is to investigate which conditions (if any) enable the flow to remain two-dimensional for $Re > 180$. We calculated two- and three-dimensional flow through periodic rotated square tube bundles with tight packing, $P/D = 1.5$, using a high resolution pseudo-spectral code with penalization. The cylinder is modelled as a rigid harmonic oscillator forced by the flow-induced lift. We find that at $Re = 200$ cylinder motion completely suppresses the three-dimensional instability. At $Re = 1000$ cylinder motion does not suppress the three-dimensional instability, although the flow does have increased spanwise correlation. The tight packing does not suppress the three-dimensional instability.

1. INTRODUCTION

The wake of an isolated cylinder first becomes three-dimensional at $Re \approx 180$ via the formation of regular streamwise vortices with a spacing of about three cylinder diameters (mode A instability). At $Re \approx 230$ a second vortex mode appears (mode B instability), characterized by irregular streamwise vortices with a spacing of one cylinder diameter (Williamson 1989). As Reynolds number increases further, the wake becomes increasingly complicated (possibly via period-doubling) until it is completely turbulent. In contrast, the transition to three-dimensionality in tightly coupled tube bundles is still not well understood. Indeed, in some experiments it appears that the flow and cylinder response remain roughly two-dimensional for Reynolds numbers well beyond 180 (Weaver 2001). For example, Price

et al. (1995) find that Strouhal frequency and rms drag do not change greatly with Reynolds number for $Re > 150$. Blevins (1985) demonstrated that acoustic forcing of an isolated cylinder at its Strouhal frequency is able to produce nearly perfect spanwise correlation of pressure for $20\,000 \leq Re \leq 40\,000$. He conjectured that similar effects might be observed in tube bundles. Blevins' investigations confirmed earlier work by Toebe (1969) who showed that a cylinder vibration amplitude of $A/D \geq 0.125$ was required to achieve a high degree of spanwise correlation. In the case of tube bundles, it has also been suggested that it is the tight spacing of the bundle that suppresses three-dimensional instability.

In this paper we attempt to understand which conditions (if any) enable the flow to remain two-dimensional for $Re > 180$. It is also possible that some aspects of the flow remain two-dimensional (e.g. spanwise correlation of vortex shedding), while others become fully three-dimensional (e.g. development of streamwise vorticity). To investigate these questions we calculate two- and three-dimensional flow through periodic rotated square tube bundles with spacing $P/D = 1.5$. We consider two types of bundles: fixed cylinder and moving cylinder bundles. The natural frequency of the moving cylinders is tuned to match the Strouhal frequency in order to maximize the moving cylinder effect. All cylinders move in phase, which corresponds to the acoustic resonance conditions investigated by Blevins (1985).

The mathematical formulation of the problem is described in §2 and the penalized pseudo-spectral method used to solve the equations is outlined in §3. Results are presented in §4, and conclusions are summarized in §5.

2. PROBLEM FORMULATION

Let us consider a viscous incompressible fluid governed by the Navier–Stokes equations

$$\frac{\partial \mathbf{u}}{\partial t} + (\mathbf{u} + \mathbf{U}) \cdot \nabla \mathbf{u} + \nabla P = \nu \Delta \mathbf{u}, \quad (1)$$

$$\nabla \cdot \mathbf{u} = 0, \quad (2)$$

where \mathbf{u} is the velocity, P is the pressure and \mathbf{U} is an imposed mean flow. We focus here on the case where the fluid occupies the complement in the plane R^3 of a periodic lattice of cylinders O_i oriented with their axes in the x_3 direction. The external boundary conditions associated with this problem are therefore that \mathbf{u} is Q -periodic on $]0, L_1[\times]0, L_2[\times]0, L_3[$, with no-slip boundary conditions on the surface of the (moving) obstacle,

$$\mathbf{u} + \mathbf{U} = \mathbf{U}_o \text{ on } \partial O_i, \quad \forall i \quad (3)$$

where \mathbf{U}_o is the velocity of the obstacle.

To model the no-slip boundary conditions without explicitly imposing (3) we follow Angot et al. (1999) by replacing (1–3) by the following set of L^2 -penalized equations

$$\begin{aligned} \frac{\partial \mathbf{u}_\eta}{\partial t} + (\mathbf{u}_\eta + \mathbf{U}) \cdot \nabla \mathbf{u}_\eta + \nabla P_\eta &= \nu \Delta \mathbf{u}_\eta \\ -\frac{1}{\eta} \chi(\mathbf{x}, t) (\mathbf{u}_\eta + \mathbf{U} - \mathbf{U}_o), & \quad (4) \end{aligned}$$

$$\nabla \cdot \mathbf{u}_\eta = 0, \quad (5)$$

where \mathbf{U}_o is the obstacle’s velocity. Note that equations (4–5) are valid in the entire domain Ω : the last term on the right hand side of (4) is a volume penalization of the flow inside the obstacle. Here $0 < \eta \ll 1$ is a penalization coefficient and χ denotes the characteristic (or mask) function

$$\chi(\mathbf{x}, t) = \begin{cases} 1 & \text{if } \mathbf{x} \in O_i, \\ 0 & \text{otherwise.} \end{cases} \quad (6)$$

Angot (1999) proved that the solution of the penalized equations (4–5) converge to that of the Navier–Stokes equations (1–2) with the correct boundary conditions (3) as $\eta \rightarrow 0$. More precisely, the upper bound on the global error of the L^2 -penalization was shown to be (Angot 1999)

$$\|\mathbf{u} - \mathbf{u}_\eta\|_{H^1(\Omega)} = O(\eta^{1/4}). \quad (7)$$

In the specific case of impulsively started flow over a plane Kevlahan and Ghidaglia (2001) showed analytically that the error in approximating (3) is actually lower: $O(\eta^{1/2})$. It seems reasonable that this is the sharp estimate in the general case as well. Note that the velocity is continuous and differentiable, due to the instantaneous

smoothing action of the Laplacian operator term (i.e. viscous diffusion).

This volume penalization has been implemented in a finite difference code (Khadra et al. 2000) for two-dimensional flow around an isolated cylinder, and was found to give good results. It is important to note that η is an arbitrary parameter, independent of the spatial or temporal discretization, and thus the boundary conditions can be enforced to any desired accuracy by choosing η appropriately. This property distinguishes the Brinkman method from other penalization schemes and allows the error to be controlled precisely.

Another advantage of the Brinkman penalization is that the force \mathbf{F}_i acting on an obstacle O_i can be found by simply integrating the penalization term over the volume of the obstacle:

$$\mathbf{F}_i = \frac{1}{\eta} \int_{O_i} (\mathbf{u}_\eta + \mathbf{U} - \mathbf{U}_o) \, d\mathbf{x}. \quad (8)$$

Thus, the calculation of lift and drag on an obstacle can be made simply, accurately and at low cost. This is helpful when calculating fluid–structure interaction, where the force must be updated at each time step. Kevlahan and Ghidaglia (2001) showed analytically that the error in calculating the force over a flat plate using (8) is only $O(\eta)$. We have found numerically that $\eta = 10^{-4}$ gives drag curves correct to about 1%.

The cylinders move as forced simple harmonic oscillators according to the equation

$$m \frac{d^2 \mathbf{x}_o}{dt^2} + b \frac{d\mathbf{x}_o}{dt} + k \mathbf{x}_o = \mathbf{F}(t), \quad (9)$$

where $\mathbf{x}_o(t)$ is the cylinder position, m is the cylinder mass, b is the damping, k is the spring constant. The fluid forcing $\mathbf{F}(t)$ is calculated as a volume integral using (8). Thus the penalized Navier–Stokes equations (4–5) are fully coupled to the cylinder motion equation (9) via the fluid force (8).

In this paper take the cylinder diameter $D = 1$, and consider square cylinder arrays where the ratio of pitch (cylinder spacing) to diameter $P/D = 1.5$ (tightly packed). This configuration models flow in the interior of a very large periodic array. The periodic domain contains only one cylinder, and thus all (image) cylinders move in phase. This corresponds to the case of acoustic resonance, caused by a standing acoustic wave between the duct walls. Although modelling all cylinders as moving in phase is unrealistic for some flows, it should maximize any suppression of three-dimensional instabilities via spanwise correlation of the vorticity.

3. NUMERICAL METHOD

The penalized Navier–Stokes equations are solved using a Fourier transform based pseudo-spectral method in space (e.g. Vincent and Meneguzzi 1991) and a Krylov method in time (Edwards et al. 1994). The pseudo-spectral method is computationally efficient and highly accurate for spatial derivatives, while the Krylov method is a stiffly stable explicit method with an adaptive stepsize to maintain error to a specified tolerance.

In the pseudo-spectral method derivatives are calculated in Fourier space with exponential accuracy, while nonlinear terms (i.e. the advection and penalization terms) are calculated in physical space. The incompressibility condition is enforced by projecting the velocity in Fourier space onto the plane normal to the wave vector \mathbf{k} . This approach has zero numerical dissipation, which is important for accurate simulation of moderate to high Reynolds number calculations. Note that although the mask is discontinuous, the velocity is continuous and differentiable. This ensures that Gibbs oscillations are small, and we have found they do not perturb the calculation, even in the vorticity formulation (Kevlahan and Ghidaglia 2001). One of the main advantages of the Brinkman penalization is that it allows us to use a Cartesian (rectangular) computational grid, which is computationally efficient. By performing grid convergence studies, we have found that a grid spacing of $h = \delta/6$ in the wall normal direction (where $\delta = Re^{-1/2}$ is the boundary layer thickness) is sufficient to give fully converged results.

The three-dimensional calculations are large ($288^2 \times 96$ grid points) and time consuming (especially at $Re = 1000$), and so we have developed a parallel version of the code. The Fourier transforms are performed using FFTW (Frigo and Johnson 1998), which parallelizes the calculation by decomposing the domain into spanwise slabs (one per processor). The Krylov time scheme is also parallelized using MPI. The resulting code scales surprisingly well for such a tightly coupled calculation: for example, each time step is 2.5 times faster on 48 processors than on 16. All parallel calculations were carried on McMaster University’s SHARCNET cluster IDRA, which has 128 processors linked by a Quadrics network.

One drawback of the penalization approach is that the small parameter η makes the equations stiff. Because of this stiffness, stepsizes are bounded by the penalization parameter, i.e.

$\Delta t \leq \eta$, unless we employ a stiffly stable method in time. To obtain an accurate force calculation we must also use a high-order method that automatically adjusts the time step to maintain the desired tolerance. We have found that the Krylov time-stepping method developed by Edwards et al. (1994) works very well for the present problem. This approach is based on the Krylov method for solving a linear system, and its accuracy (in the linear case) is $O(K)$, where K is the dimension of the Krylov subspace used to approximate the matrix representing the right hand side of the equation. The step size is set to ensure that the L^2 error in the approximation of $\partial\mathbf{u}/\partial t$ is smaller than the desired tolerance. This is done by comparing the exact value for $\partial\mathbf{u}/\partial t$ (given by the right hand side of the equation) to the approximation to $\partial\mathbf{u}/\partial t$ given by differentiating the Krylov approximation to $\mathbf{u}(t)$. We have found that the Krylov approach gives good results, especially when the cylinder is moving. In our calculations we use $K = 10$, and set the L^2 error tolerance to 10^{-3} . With these parameters we achieve a CFL value of 2 to 6.

To eliminate noise in the force calculation when the cylinder is moving which is caused when grid points move in or out of the mask, we slightly smooth the edge of the mask. The mask is smoothed over a distance of only $h/6$ (i.e. $1/6$ of a grid point). This smoothing completely eliminates the noise, and changes the force by less than 1%. One can view this slight smoothing as rounding the step-like edge of the cylinder due to the Cartesian grid approximation of its boundary.

4. RESULTS

In each of the following cases we do four simulations: two-dimensional with fixed and moving cylinders, and three-dimensional with fixed and moving cylinders. This allows us to directly compare the two- and three-dimensional flows in order to determine the degree of suppression of three-dimensional instability. The Reynolds number is defined as $Re = |\mathbf{U}|D/\nu$ ($|\mathbf{U}| = D = 1$), and the flow is at 45° to the axis of the square cylinder array (this is referred to as a *rotated square* array). The computational domain contains one cylinder and has dimensions $L_1 \times L_2 = 1.5 \times 1.5$ in the plane perpendicular to the cylinder axis. In each case the spring constant is chosen to match the Strouhal frequency of the fixed two-dimensional cylinder, the cylinder is undamped ($b = 0$), and the total mass

Case	Peak frequency
2D, fixed	1.32
2D, moving	0.95
3D, fixed	1.18
3D, moving	0.95

Table 1: Peak lift frequencies at $Re = 200$.

(mass plus added mass) $m_* = 5$.

4.1. Reynolds number 200

The computational grid is $128^2 \times 64$, and the length of the domain in the spanwise direction is 6 (sufficient to capture the streamwise vorticity, which has a wavelength of about 3D). Although the spanwise direction is not as finely resolved as the other directions ($h = 3/4\delta$, compared with $h = \delta/6$ for the other directions), we have checked *a posteriori* that three-dimensional vorticity is sufficiently well resolved. This is actually slightly more than the spanwise resolution used in the finite volume calculations of Persillon and Braza (1998). The normalized spring constant set to $k_* = 451.1$ in order to match the Strouhal frequency $f = 1.32$ of the fixed two-dimensional cylinder.

Figure 1 shows the lift curves at short and long times for the fixed and moving cylinders. In both cases the lift curves agree at short times (before the three-dimensional instability has developed). However, at longer times the three-dimensional fixed cylinder's lift amplitude is modulated in a non-stationary way, whereas the the moving cylinder's lift still closely matches that of the moving two-dimensional cylinder. Table 1 lists the peak lift frequencies for each of the cases. The frequencies of the two- and three-dimensional moving cylinder cases match, while those of the fixed cases differ by about 9%.

It is clear from figure 2(c) that the moving cylinder completely suppresses the production of streamwise vorticity, while figure 2(a) shows the development of streamwise vortices at a spacing of about 1.8D, slightly closer than seen in simulations of flow past isolated cylinders (Persillon and Braza 1998). Finally, figure 2(b) shows that, although significant streamwise vorticity has been generated, the spanwise vorticity is still largely two-dimensional except for some perturbation at the trailing edge of the vortex sheets due to interaction with the streamwise vortices.

These results show that at $Re = 200$ in-phase ‘acoustic resonance’ movement of the cylinders completely suppresses the development of any

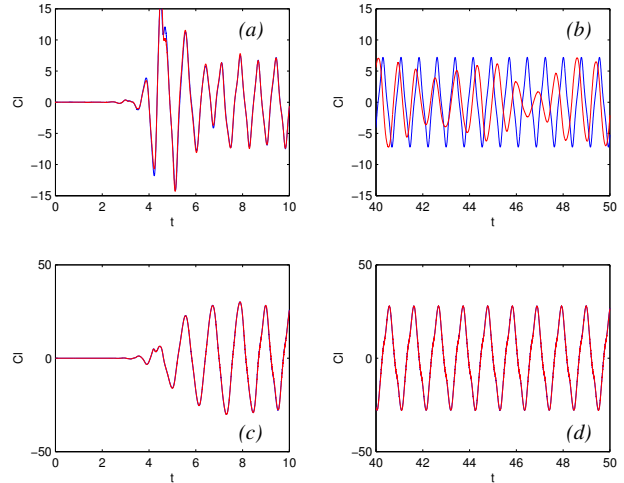


Figure 1: Lift curves for $Re = 200$ case. (a) Fixed cylinder, short times: 2D and 3D results match. (b) Fixed cylinder, long times: 2D has fixed amplitude, while 3D has modulated amplitude. (c) Moving cylinder, short times: 2D and 3D results match. (d) Moving cylinder, long times: 2D and 3D results match.

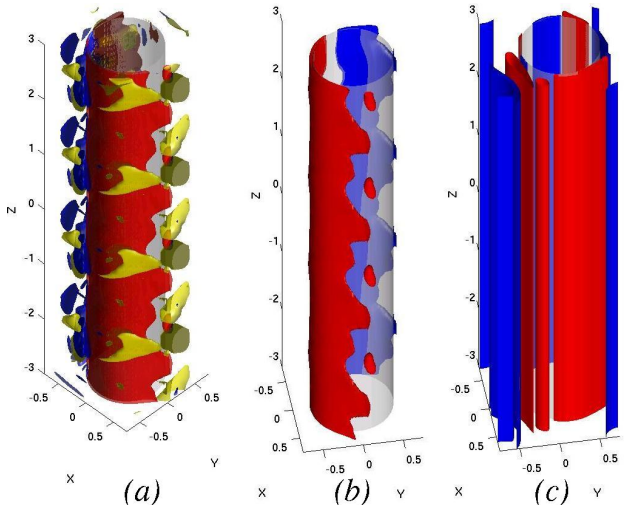


Figure 2: Isosurfaces of three-dimensional vorticity at $t = 50$ for $Re = 200$. (a) Fixed cylinder, three components. (b) Fixed cylinder, spanwise vorticity. (c) Moving cylinder, spanwise vorticity.

three-dimensionality in the flow. Since the amplitude of cylinder oscillation is $A/D = 0.23 > 0.125$, these results are consistent with the observations of Toebes (1969) that sufficiently large amplitude cylinder vibration amplitude should produce a high degree of spanwise correlation. We also find that the tight packing alone does not suppress three-dimensional instabilities.

4.2. Reynolds number 1 000

In this section we present some preliminary results for the $Re = 1000$ case. We found that we needed to increase the spanwise resolution to $h = \delta/2$, and these results were calculated at the lower streamwise plane resolution of $h = \delta/4$. The computational grid is $192^2 \times 96$, and the length of the domain in the spanwise direction is 1.5 (i.e. the domain is cubic). As we will see, the shorter spanwise domain is sufficient due to the smaller size of the streamwise vortices at this Reynolds number. The normalized spring constant set to $k_* = 259.4$ in order to match the peak Strouhal frequency $f = 1.00$ of the fixed two-dimensional cylinder.

The drag and lift curves shown in figure 3 demonstrate that the three-dimensional forces are decorrelated from the two-dimensional forces and are of much lower amplitude for both the fixed and moving cylinder cases. The lower amplitude in the three-dimensional flow is likely due to the disorganized streamwise and transverse vorticity generated by the (unsuppressed) three-dimensional instability (see figure 3). However, figures 3(a) and (d) indicated that cylinder movement does increase the spanwise correlation of spanwise vorticity. The lack of suppression of the three-dimensional instability is consistent with the fact that, as shown in figure 5, the cylinder vibration amplitude is only $A/D \approx 0.05$, which is less than the minimum threshold of 0.125 identified by Toebes (1969). Somewhat surprisingly, as shown in table 2, the peak Strouhal frequency of the fixed three-dimensional cylinder is equal to the average of the two peaks of the two-dimensional cylinder, while the peak Strouhal frequencies of the moving two- and three-dimensional cylinders differ by 13%. These results appear to indicate that tuning the cylinder response to the Strouhal frequency of the fixed cylinder does not produce sufficiently large cylinder vibrations to suppress the three-dimensional instability.

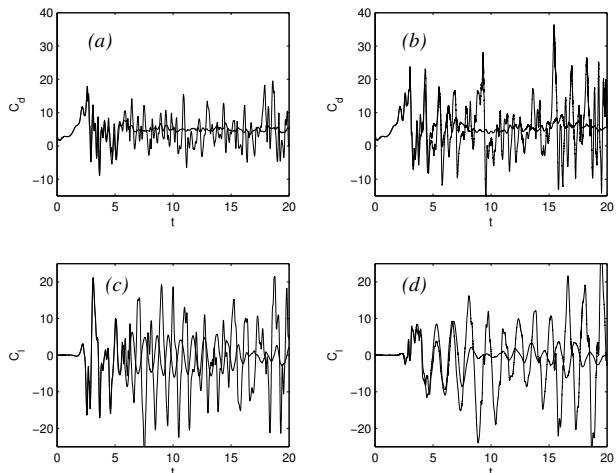


Figure 3: Drag and lift at $Re = 1000$ case. In each figure the three-dimensional curve is the one with the lower amplitude. (a) Drag, fixed cylinder. (b) Drag, moving cylinder. (c) Lift, fixed cylinder. (d) Lift, moving cylinder.

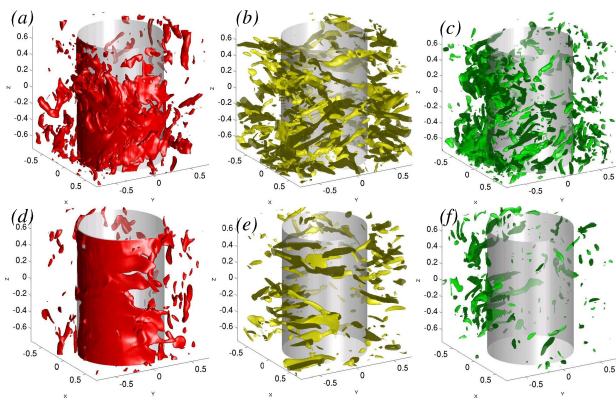


Figure 4: Isosurfaces of three-dimensional vorticity at $t = 15$ for $Re = 1000$. (a) Fixed cylinder, spanwise vorticity. (b) Fixed cylinder, streamwise vorticity. (c) Moving cylinder, transverse vorticity. (d) Moving cylinder, spanwise vorticity. (e) Moving cylinder, streamwise vorticity. (f) Moving cylinder, transverse vorticity.

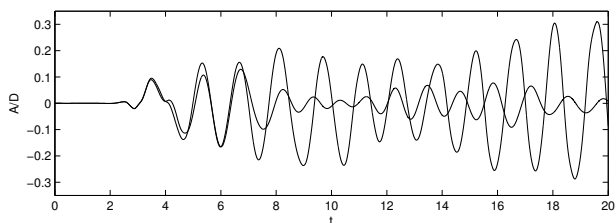


Figure 5: Cylinder amplitude at $Re = 1000$.

Case	Peak frequency
2D, fixed	0.8, 1.15 (two peaks)
2D, moving	0.70
3D, fixed	0.98
3D, moving	0.79

Table 2: Peak lift frequencies at $Re = 1000$.

5. CONCLUSIONS

We have used high resolution penalized pseudo-spectral simulations to investigate how and when in-phase cylinder vibration of tube bundles can suppress three-dimensionality. The in-phase cylinder vibration models the case of acoustic resonance, which was observed by Blevins (1985) to induce nearly perfect spanwise correlation of pressure. We performed two- and three-dimensional simulations of fixed and moving tube bundles at the relatively low Reynolds number $Re = 200$ (when only the mode A instability is present), and the moderate Reynolds number $Re = 1000$ when the flow around the fixed cylinder is highly three-dimensional and the three-dimensional instability is more complicated and much stronger.

We found that at $Re = 200$ the cylinder vibration is large enough ($A/D = 0.23 > 0.125$) to completely suppress the three-dimensional instability. The Strouhal frequency of the moving three-dimensional cylinder is the same as that of the moving two-dimensional cylinder, and no streamwise or transverse vorticity is produced. Note that the tight packing $P/D = 1.5$ of the tube bundle is not sufficient by itself to suppress the three-dimensional instability.

In contrast, at $Re = 1000$ the cylinder vibration is insufficient ($A/D \approx 0.05 < 0.125$) to suppress the three-dimensional instabilities, although the spanwise vorticity is slightly more correlated. This may be due to the fact that significant transverse and streamwise vorticity, which is uncorrelated in the spanwise direction, is generated before the cylinder vibration is large enough to suppress the three-dimensional instability. This result does not agree with Blevins (1985)'s observation that acoustic forcing at the Strouhal frequency should correlate the flow in the spanwise directions, even at $20000 \leq Re \leq 40000$. In this case the tight packing of the tube bundle may actually reduce the cylinder vibration amplitude compared to the single cylinder case considered by Blevins. These results still need to be confirmed by a higher resolution simulation.

Acknowledgements

The authors gratefully acknowledge the use of SHARCNET's parallel computers. JS and NT were supported by SHARCNET undergraduate fellowships during this work, and NKRK's research is supported by NSERC.

6. REFERENCES

- P. Angot. Analysis of singular perturbations on the brinkman problem for fictitious domain models of viscous flows. *Mathematical Methods in the Applied Science*, 22:1395–1412, 1999.
- P. Angot, C.-H. Bruneau, and P. Fabrie. A penalization method to take into account obstacles in viscous flows. *Numerische Mathematik*, 81:497–520, 1999.
- R.D. Blevins. The effect of sound on vortex shedding. *J. Fluid Mech.*, 161:217–237, 1985.
- W. S. Edwards, L. S. Tuckerman, R. A. Friesner, and D. C. Sorensen. Krylov methods for the incompressible navier–stokes equations. *J. Comp. Phys.*, 110:82–102, 1994.
- M. Frigo and S. G. Johnson. FFTW: an adaptive software architecture for the FFT. In *ICASSP conference proceedings*, volume 3, pages 1381–1384, 1998.
- N. Kevlahan and J.-M. Ghidaglia. Computation of turbulent flow past an array of cylinders using a spectral method with brinkman penalization. *Eur. J. Mech./B*, 20:333–350, 2001.
- K. Khadra, P. Angot, S. Parneix, and J. P. Caltagirone. Fictitious domain approach for numerical modelling of navier-stokes equations. *Int. J. Num. Meth. Fluids*, 34:651–684, 2000.
- H. Persillon and M. Braza. Physical analysis of the transition to turbulence in the wake of a circular cylinder by three-dimensional navier–stokes simulation. *J. Fluid Mech.*, 365:23–88, 1998.
- S. J. Price, M. P. Païdoussis, and B. Mark. Flow visualization of the interstitial cross-flow through parallel triangular and rotated square arrays of cylinders. *J. Sound and Vibration*, 181:85–98, 1995.
- G.H. Toebes. The unsteady flow and wake near an oscillating cylinder. *Trans. ASME D: J. Basic Engng.*, 91:493–498, 1969.
- A. Vincent and M. Meneguzzi. The spatial structure and statistical properties of homogeneous turbulence. *J. Fluid Mech.*, 225:1–20, 1991.
- D. S. Weaver. private communication, 2001.
- C. H. K. Williamson. Oblique and parallel modes of vortex shedding in the wake of a circular cylinder at low reynolds numbers. *J. Fluid Mech.*, 206:579–627, 1989.